Heliyon 9 (2023) e21170

Contents lists available at ScienceDirect

Heliyon

journal homepage: www.cell.com/heliyon

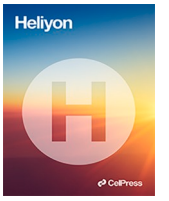

AGEs induce high expression of Dll4 via endoplasmic reticulum stress PERK signaling-mediated internal ribosomal entry site mechanism in macrophages

Yanpeng Ma [a,b,c,1], Shixiang Zheng [d,1], Xiqiang Wang [a,b,c], Ling Zhu [a,b,c], Junkui Wang [a,b,c], Shuo Pan [a,b,c], Yong Zhang [a,b,c], Zhongwei Liu [a,b,c,*]

[a] *Department of Cardiology, Shaanxi Provincial People's Hospital, Xi'an, 710068, China*
[b] *Atherosclerosis Integrated Chinese and Western Medicine Key Research Laboratory, Research Office of Shaanxi Administration of Traditional Chinese Medicine, Xi'an, 710003, China*
[c] *Affiliated Shaanxi Provincial People's Hospital, Northwestern Polytechnical University, Xi'an, 710068, China*
[d] *Department of Critical Medicine, Fujian Medical University Union Hospital, Fuzhou, 350000, China*

ARTICLE INFO

Keywords:
Advanced glycation end products
Macrophages
Delta-like 4 ligand
Internal ribosome entry site

ABSTRACT

Background and aim: Advanced glycation end products (AGEs)- exposed macrophages was characterized by Delta-like ligand 4 (Dll4) high expressed and has been shown to participate in diabetes-related atherosclerosis. This study was aimed to investigate the translational regulatory mechanism of Dll4 high expression in macrophages exposed to AGEs.

Methods: Human Dll4 5′ untranslated region (5′UTR) sequence was cloned and inserted into a bicistronic reporter plasmid. Human THP-1 macrophages transfected with the bicistronic reporter plasmids were exposed to AGEs. Dual-luciferase assay was used to detect internal ribosome entry site (IRES) activity contained in Dll4 5′UTR. Small interference RNA transfection was used to knock-down specific gene expression. Localization of protein was analyzed.

Results: AGEs exposure significantly induced IRES activity in Dll4 5′ UTR in human macrophages. Internal potential promoter and ribosome read-through mechanisms were excluded. Inhibition of endoplasmic reticulum stress and specific silencing of protein kinase R-like endoplasmic reticulum kinase (PERK)/eukaryotic initiation factor 2α (eIF2α) signaling pathway activation reduced IRES activity in Dll4 5′ UTR in human macrophages. Dll4 5′ UTR IRES activity was also inhibited by targeted silencing of heterogeneous nuclear ribonucleoprotein A1 (hnRNPA1). Moreover, specific inhibition of PERK/eIF2α signaling pathway led to deactivation of hnRNPA1, resulting to reduction of AGEs- induced Dll4 5' UTR IRES activity in human macrophages.

Conclusions: AGEs induced Dll4 5′ UTR IRES activity in human macrophages which was dependent on endoplasmic reticulum stress PERK/eIF2α signaling pathway. hnRNPA1 acted the role as an ITAF was also indispensable for AGEs-induced Dll4 5′UTR IRES activity in human macrophages.

* Corresponding author. Department of Cardiology, Shaanxi Provincial People's Hospital, 256 Youyi Xi Rd, Xi'an, Shaanxi Province, 710068, China.
E-mail address: liuzhongwei@nwpu.edu.cn (Z. Liu).
[1] These authors contributed equally to this work.

https://doi.org/10.1016/j.heliyon.2023.e21170
Received 17 May 2023; Received in revised form 14 October 2023; Accepted 17 October 2023
Available online 18 October 2023

1. Introduction

Macrovascular complications take major responsibility for the mortality in patients with type 2 diabetes mellitus (T2DM). Atherosclerosis is one of the recognized pathological features of T2DM macrovascular complications. Meanwhile, T2DM has been identified as a risk factor of atherosclerosis. Ours and others' previous investigations suggested the progression of atherosclerosis was accelerated in T2DM patients [1,2].

Advanced glycation end products (AGEs) are characterized toxic metabolites of T2DM [3]. It was reported AGEs were largely produced in individual with T2DM and associated with promoted atherosclerotic plaque growth and rupture [4]. Atherosclerosis could be recognized as the chronic inflammation occurs within the arterial wall. Among involved immune cells, macrophages play critical roles in formation and development of atherosclerotic lesions [5].

It is now accepted that M1 polarized macrophages contribute to aggravation of atherosclerosis due to their pro-inflammatory roles [6]. M1 macrophage-mediated vascular smooth muscle cells (VSMCs) contractile -to - synthetic phenotypic conversion was one of the fundamental underlying mechanisms of atherosclerosis [1]. According to our previous studies, these M1 macrophages were characterized by high expression of Delta-like 4 ligand (Dll4) which further activated Notch pathway to induce phenotypic conversion of VSMCs by direct cell-to-cell contact [1,7].

According to our previous investigation, AGEs facilitated macrophage M1 polarization via receptor for AGEs (RAGE) signaling pathway which further mediated reactive oxygen species (ROS) production via NADPH oxidase [8,9]. Under sustained AGEs- induced ROS stimulation, endoplasmic reticulum (ER) stress is triggered [10]. The translational process of many gene expression is suspended due to the initiation of unfolded protein response (UPR) under circumstance of ER stress [11]. The regulation of Dll4 expression has been well-studied at transcriptional and post-transcriptional levels [12]. Thus, it is reasonable for us to speculate if there exist alternative regulatory mechanisms except for transcriptional and post-transcriptional ones. In this study, at the translational level, we tried to identify an internal ribosome entry site (IRES) in the 5′ untranslated regions (5′UTR) of Dll4 mRNA under the condition of ER stress.

2. Materials and methods

2.1. Preparation of AGEs-bovine serum albumin (BSA)

To prepare Advanced Glycation End-products Bovine Serum Albumin (AGEs-BSA), we meticulously followed an optimized protocol building on our previous work [8]. Briefly, BSA (Hyclone) was first dissolved in a sodium phosphate ($NaPO_4$) buffer solution with a concentration of 0.2 mmol/L and a pH of 7.4. To this solution, we added glyceraldehyde (Merck) at a concentration of 0.1 mmol/L. Ensuring sterility, the mixture was then incubated at a consistent temperature of 37 °C for a duration of 7 days to facilitate the formation of AGEs. After this period, to purify our AGEs-BSA and separate it from any unincorporated sugars, we utilized a thorough dialysis approach. The samples were transferred to a PD-10 desalting column (GE HealthCare). Dialysis was performed in PBS, maintained at a cool 4 °C, for a 24-h period. To ensure the maximum removal of residual sugars, the PBS buffer was refreshed three times during the dialysis process. Once dialysis was complete, AGEs-BSA samples were carefully collected and stored for subsequent analyses. As a benchmark, BSA that had not been treated with glyceraldehyde was prepared and served as our control sample.

2.2. Cell culture

The THP-1 human monocytic cell line was obtained from the Cell Bank of the Chinese Academy of Sciences (Shanghai, China). THP-1 cells were differentiated into macrophage-like cells using phorbol myristate acetate (PMA). Cells were treated with 100 ng/mL PMA (Sigma-Aldrich) for 72 h. Differentiated cells were seeded in RPMI-1640 medium (Hyclone) enriched with 10 % fetal bovine serum (FBS, Hyclone). To minimize the risk of microbial contamination, the medium was supplemented with a 1 % antibiotic mixture containing penicillin and streptomycin (Abcam). The cells were cultured in a humidified incubator set at an atmosphere of 5 % CO_2 and 95 % air, with a consistent temperature of 37 °C. Regular cell culture protocols were adhered to, ensuring optimal cell growth and maintenance.

Table 1
Oligonucleotide primers used in RT-PCR.

Primer	Forward (5′-3′)	Reverse (5′-3′)
dll4 5′UTR	AAACTAGTGCTGCGCGCAGGCCGGGAACACG	AAAACCATGGCCCCTCGGGCGTCGCTCTCTC
dll4	AGAGGAGAAGGAGGAGGAATG	CCCTTGACTCTTCCCTTGATG
perk	GCGGCAATGAGAAGTGGAAT	TCCCTCTGGGCTTAAAGGTG
eif2α	CTCCTGAAAGCAGCAACCTC	GACCGAGATGAAGCATCGTG
hnrnpa1	TGCCCAGAAAATGAAAAAGG	GTGTATGTGGCAATGCGTTC
gapdh	CAAGGTCATCCATGACAACTTTG	GTCCACCACCCTGTTGCTGTAG

2.3. Plasmid constructs and transfection

For plasmid construction, the 5′UTR of human Dll4, spanning nucleotides 1 to 320, was amplified using polymerase chain reaction (PCR). Primer sequences utilized for this amplification are detailed in Table 1. Resultant PCR products underwent purification and were subsequently subcloned into the Zero Blunt™ shuttle vector (ThermoFisher). DNA sequencing was employed to verify the accuracy of these sequences. Separately, the pRF plasmid, derived from pGL3 (Promega) and equipped with Ned I and *Eco*R I restriction sites, was custom-synthesized by GenePharma. This led to the construction of three specific plasmids based on the pRF backbone: 1) The Dll4 5′-UTR fragment was ligated into the intercistronic region of pRF, resulting in the pRL-dll4-FL construct. 2) A modified pRF plasmid, devoid of the SV40 promoter sequence (termed δpRF), was synthesized. The Dll4 5′ UTR fragment was integrated into this plasmid to yield δpRL-dll4-FL. 3) A hairpin structure sequence (5′-CCCGGAGCGCCCAGATCTGGGCGCTCCGGGGTAC-3′) was positioned upstream of RL. Following this, the Dll4 5′-UTR fragment was integrated to produce hpRL-dll4-FL. The schematic representations of these constructs can be found in Fig. 1. For cell transfection, plasmids were introduced into macrophages using the Lipofectamine™ Reagent (Invitrogen). A ratio of 2 μL Lipofectamine™ reagent to 2 μg of plasmid was maintained for each well during the transfection procedure.

2.4. siRNA transfection

RNA interference (RNAi) was employed to selectively knock down the expression of protein kinase R-like endoplasmic reticulum kinase (PERK), eukaryotic initiation factor 2α (eIF2α), and heterogeneous nuclear ribonucleoprotein A1 (hnRNPA1). Specific small interfering RNAs (siRNAs) targeting these genes were custom-designed, evaluated for efficiency, and synthesized by GenePharma. The precise sequences targeting PERK, eIF2α, and hnRNPA1 are provided in Table 2. For the transfection process, macrophages were exposed to the synthesized siRNAs at a concentration of 20 μmol/L. The Lipofectamine™ reagent (Invitrogen) was used as the transfection agent, with an optimized ratio of 2 μL Lipofectamine™ to 1.5 μL siRNA for each well to ensure maximum siRNA uptake and gene silencing efficiency.

2.5. Cells treatment

Macrophages in culture underwent stimulation with AGEs at concentrations of 2.5, 5.0, 7.5, and 10.0 μg/mL, with an exposure duration of 48 h. Subsets of these macrophages were subjected to specific pretreatments to assess the effects of various modulators. One subset was exposed to the ER stress inhibitor 4-phenylbutyrate (4-PBA) at a concentration of 1.0 mmol/L for 24 h. Another subset received treatment with the RAGE inhibitor FPS-ZM1 (Beyotime) at a dose of 1 μmol/L for a 24-h period, as referenced [13]. To investigate the effects of genetic modulation, certain macrophages were transfected with specific plasmids and/or siRNAs, and this transfection was performed 12 h prior to their exposure to AGEs.

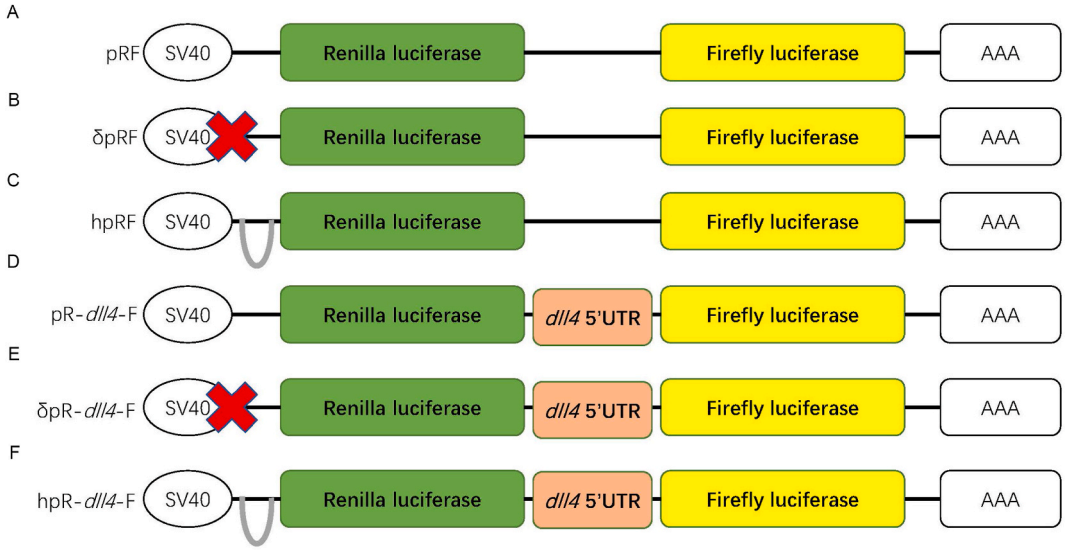

Fig. 1. Detailed Schematic of Bicistronic Reporter Plasmids Utilized. The illustration showcases the structural configurations of six distinct bicistronic reporter plasmids used in our study. **(A) pRF** represents a standard bicistronic construct housing both Firefly (FL) and Renilla (RL) luciferase genes, demarcated by an intercistronic sequence. **(B) δpRF** is a derivative of the pRF, distinguished by the absence of the SV40 promoter sequence, leading to an altered transcriptional landscape. **(C) hpRF** incorporates a unique hairpin structure sequence positioned upstream of the RL gene, influencing its expression dynamics. **(D) pR-dll4-F**, **(E) δpR-dll4-F**, and **(F) hpR-dll4-F** are specialized constructs, each harboring the Dll4 5′-UTR fragment at strategic locations, designed to elucidate its role in modulating luciferase gene expression under varying cellular conditions.

Table 2
siRNA sequences.

Target gene	sense (5′-3′)	antisense (5′-3′)
perk	GGACGAUCCUGCUUUGCAUTT	AUGCAAAGCAGGAUCGUCCTT
eif2α	CCCAGGUAUGUGAUGACAATT	UUGUCAUCACAUACCUGGGTT
hnrnpa1	GAGAUGGCUAGUGCUUCAUTT	AUGAAGCACUAGCCAUCUCTT

2.6. Luciferase assay

Luciferase activity was quantitatively assessed using the Dual-Luciferase Reporter Assay kit (Promega), with procedures meticulously adhering to the manufacturer's guidelines. Post-transfection (48 h), both Firefly (FL) and Renilla (RL) luciferase signals were detected and quantified. For this purpose, a Varioskan LUX luminometer (ThermoFisher) was employed, ensuring precise measurement of the respective luciferase activities.

2.7. Immunofluorescent stains

Cells adhered to cover glass underwent fixation using 4 % paraformaldehyde. Following a thorough wash with PBS and an incubation step with blocking buffer, these fixed cells were probed with hnRNPA1 antibody (1:200 dilution, Abcam, #ab177152) in a controlled environment at 4 °C for a duration of 8 h. For visualization, cells were then exposed to Alexa Fluor 555-conjugated secondary antibodies at room temperature (approximately 25 °C) for 1 h. The cell nuclei were distinctly marked using 4,6-diamidino-2-phenylindole (DAPI, Abcam, #ab285390). High-resolution imaging was achieved using a fluorescence microscope, specifically the Axio Imager 2 model (Zeiss). To determine the degree of co-localization between hnRNPA1 (highlighted by Alexa Fluor-555) and DAPI, Image J software (version 1.53t) was employed, alongside its plugin, Coloc 2. Quantitative assessment of this co-localization was determined through the Pearson's R value.

2.8. Real-time PCR

Expression levels of perk, eif2α, hnrnpa1, and dll4 in THP-1 cells were ascertained through quantitative real-time PCR. Total RNA from macrophages was isolated employing the TRIzol kit (TaKaRa). This extracted RNA underwent subsequent reverse transcription into cDNA using the SuperScript™ III reverse transcriptase kit (Invitrogen). The integrity, purity, and concentration of the resultant cDNA were rigorously assessed via NanoDrop spectrophotometer (Thermo). Primers used for the amplification process are detailed in Table 1. Quantitative amplification was executed utilizing the SYBR Green Fluorescein qPCR Master Mix (ThermoFisher). The ViiA 7 Quantitative PCR system (Applied Biosystems) was employed to calculate relative mRNA expression levels, with quantification achieved using the $2^{-\triangle\triangle Ct}$ method.

2.9. Western blotting

Cells, once harvested, were subjected to lysis using the radioimmunoprecipitation assay (RIPA) buffer system (Santa Cruz), complemented with phenylmethylsulfonyl fluoride (PMSF) (Santa Cruz). For protein extractions, three distinct kits were employed: the Total Protein Extraction Kit (Beyotime) for comprehensive protein extraction, the Cytoplasmic Protein Extraction Kit (Beyotime) specifically for cytoplasmic proteins, and the Nuclear Protein Extraction Kit (Beyotime) to isolate nuclear proteins. Protein concentrations were accurately determined using a BCA kit (Invitrogen). Proteins were then resolved via sodium dodecyl sulfate polyacrylamide gel electrophoresis (SDS-PAGE) and subsequently transferred to polyvinylidene fluoride (PVDF) membranes through electroblotting. Post-transfer, membranes were blocked using QuickBlock™ buffer (Beyotime) before incubation with primary antibodies targeting PERK (1:1000, Abcam, #ab229912), phosphorylated PERK (p-PERK, 1:500, Abcam, #ab192591), eIF2α (1:1000, CST, #5324S), phosphorylated eIF2α (*p*-eIF2α, 1:500, CST, #3398S), hnRNPA1 (1:500, Abcam, #ab177152), Histone H3 (1:2000, Abcam, #ab1791), and glyceraldehyde 3-phosphate dehydrogenase (GAPDH) (1:2000, Abcam, #ab8245). This incubation was conducted at 4 °C for a duration of 10 h. Subsequent to primary antibody binding, membranes were washed with Tris-buffered saline with Tween 20 (TBST) and incubated with horseradish peroxidase (HRP)-conjugated secondary antibodies (Abcam, #ab97080) at room temperature for 2 h. Detection was facilitated using an enhanced chemiluminescence (ECL) kit (Invitrogen), with protein bands visualized on X-ray films.

3. Statistics

Data was presented in a (mean ± standard deviation) manner. Number of independent experiments was "n". Comparisons of differences between two groups were carried out by one-way analysis of variance (ANOVA). Bunnett's test or Bonferroni test were carried out as post-hoc test. When $P < 0.05$, the compared differences were considered as statistically different.

4. Results

4.1. AGEs induced Dll4 expression in cultured THP-1 cells at post-transcriptional level

Results from our previous study indicated that AGEs induced high expression of Dll4 in mice primary macrophages [1]. As shown in Fig. 2A, the alteration of Dll4 mRNA was not significant in THP-1 cells incubated with AGEs. As shown in Fig. 2B, AGEs stimulation significantly increased Dll4 expression in human THP-1 macrophages in an AGEs concentration-dependent manner. These results indicated that the up-regulation of Dll4 expression was post-transcriptional. Generally, under circumstance of sustained ER stress, the cap-dependent translation would be suspended. Thus, we proposed that 5′UTR of Dll4 contained IRES elements.

4.2. A functional IRES was identified in human Dll4 5′UTR in THP-1 cells

The 5′UTR of human Dll4 was listed according to the database of GenBank (NM_019074.4). The RNA sequence contains 320 nts with GC composition of 70 % (Fig. 3A). According to RNA Folding Form online software (Ver 2.3), the 5′UTR of Dll4 could form stable and complex RNA secondary structures ($\Delta G = -59.00$ kcal/mol, Fig. 3B). In this study, dual-luciferase reporter assay was used to evaluate the IRES activity in Dll4 5′UTR. The reporter plasmid pRL-dll4-FL was transfected to THP-1 cells. Activities of RL and FL were detected. The increase of FL/RL indicated IRES activity. As shown in Fig. 3C, compared with negative control, FL/RL dramatically increased in THP-1 cells exposed to AGEs. These results indicated there was a functional IRES in human Dll4 5′UTR.

4.3. Characteristics of IRES located in human Dll4 5′UTR

The dual-luciferase reporter assay could be false positive due to alternative mechanisms including internal potential promoter and ribosomal read-through. In order to exclude internal potential promoter, the reporter plasmid δpRL-dll4-FL was transfected in to THP-1 cells. The SV40 promoter sequence was deleted in this plasmid. As shown in Fig. 4A, no RL nor FL activities was detected in THP-1 cells exposed to AGEs, indicating there were no internal potential promoter inside Dll4 5′UTR. In order to exclude ribosomal read-through, the reporter plasmid hpRL-dll4-FL was transfected into THP-1 cells. A harpin sequence was added to inhibit RL activity. As shown in Fig. 4B, RL activity in AGEs-exposed THP-1 cells transfected with hpRL-dll4-FL was decreased significantly compared with cells transfected with pRL-dll4-FL. Moreover, difference of FL activities between AGEs-exposed THP-1 cells transfected with hpRL-dll4-FL and pRL-dll4-FL was not significant, indicating FL activity was not mediated by ribosome read-through mechanism.

4.4. Dll4 IRES activity was activated by AGEs/RAGE-induced ER stress

THP-1 cells transfected with pRL-dll4-FL were pre-treated with ER stress inhibitor 4-PBA or RAGE inhibitor FPS-ZM1 prior to AGEs exposure. ER stress was evaluated by the expression of its hall marker GRP78. As demonstrated in Fig. 5A, FPS-ZM1 pre-treatment significantly reduced Dll4 protein expression level without affecting Dll4 mRNA level in macrophages exposed to AGEs. As shown in Fig. 5B, 4-PBA pre-treatment reduced Dll4 protein expression level without significant impact on Dll4 mRNA expression level in human macrophages exposed to AGEs. As shown in Fig. 5C, AGEs exposure dramatically increased FL/RL in THP-1 cells. 4-PBA pre-treatment, however, decreased FL/RL in THP-1 cells exposed to AGEs. As demonstrated in Fig. 5D, AGEs exposure significantly elevated GRP78 expression which was decreased by 4-PBA pre-treatment. These results indicated that the Dll4 5′UTR IRES activity was dependent on ER stress which was induced by AGEs/RAGE activation.

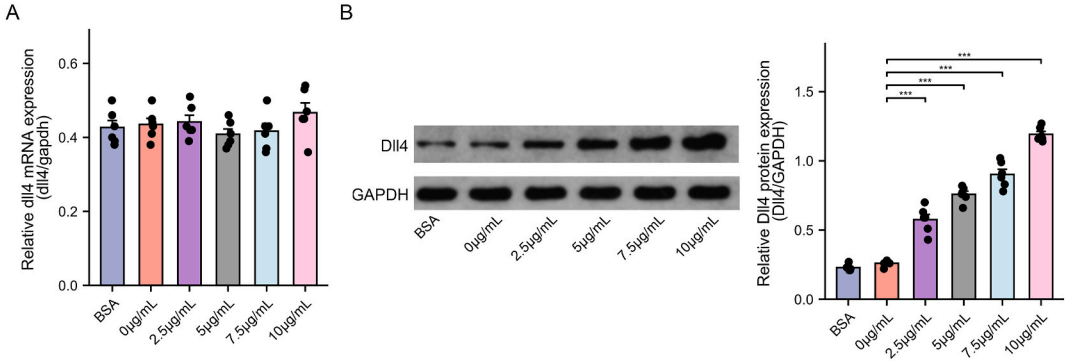

Fig. 2. Analysis of Dll4 Expression in THP-1 Macrophages Following AGEs Exposure. (A) A bar graph representing the relative mRNA expression levels of dll4 in THP-1 macrophages post exposure to AGEs at concentrations of 0, 2.5, 5.0, 7.5, and 10.0 μg/mL over a 48-h period. **(B** and FigureS1) Immunoblots displaying the protein profiles of Dll4 and the housekeeping protein, GAPDH, as controls. Accompanying bar graphs further quantify the relative protein expression levels of Dll4 in THP-1 macrophages under identical AGEs exposure conditions as described in **(A)**. (n = 6, *P < 0.05, **P < 0.01, ***P < 0.001).

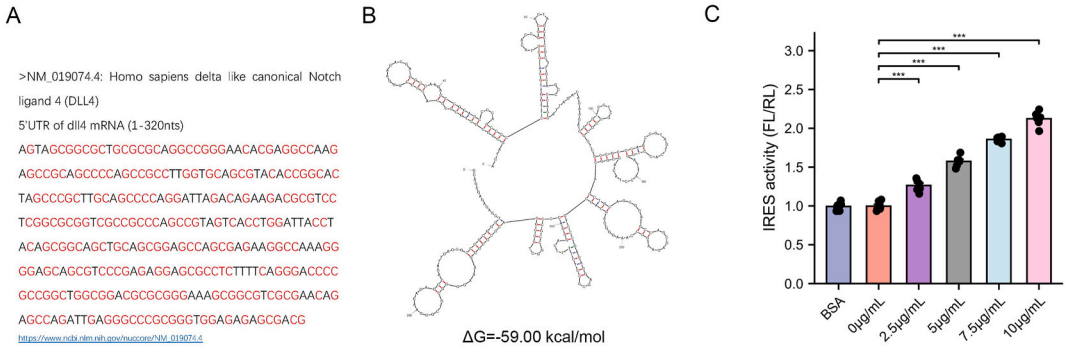

Fig. 3. Analysis and Structural Insights into the 5′UTR of Dll4 mRNA and its IRES Activity in the Context of AGEs Exposure. (A) Depicts the nucleotide sequence of the 5′UTR region of dll4 mRNA. Nucleotides 'G' and 'C' are highlighted in red, underscoring the GC-rich nature of this region with a notable GC content of 70 %. **(B)** The predicted secondary structure of the human Dll4 mRNA 5′UTR, generated using the Form online software (Version 2.3). This visualization aids in understanding the potential conformational intricacies of the 5′UTR region, which could have implications for its translational regulation. **(C)** Bar chart representation of the IRES activity (as gauged by the FL/RL ratio) associated with the Dll4 mRNA 5′UTR in human macrophages subjected to AGEs at concentrations of 0, 2.5, 5.0, 7.5, and 10.0 μg/mL (n = 6, *P < 0.05, **P < 0.01, ***P < 0.001).

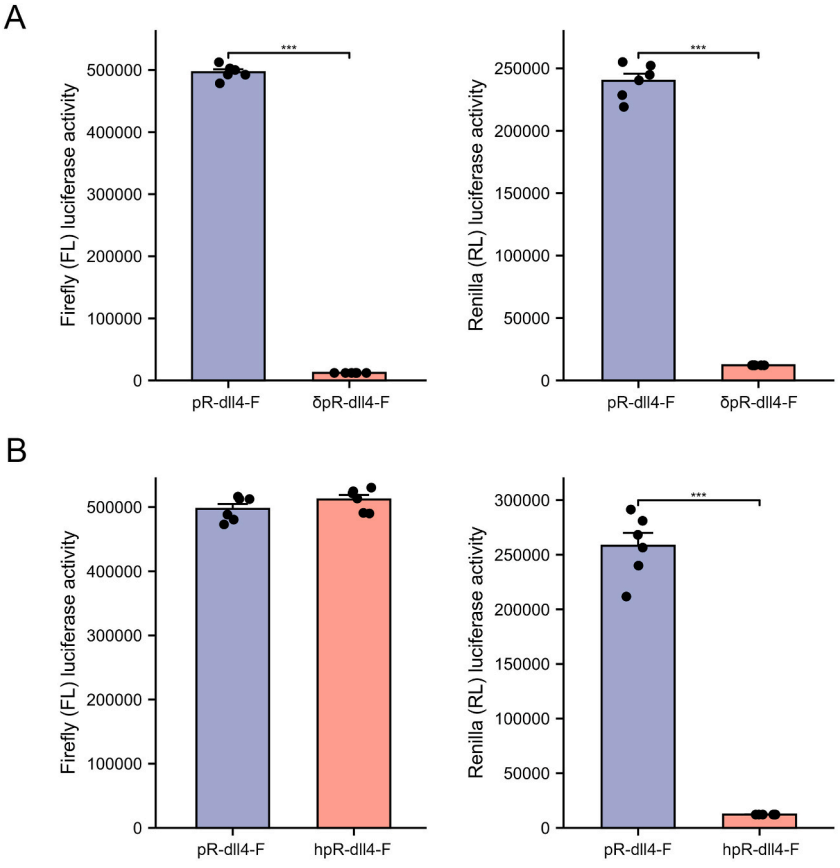

Fig. 4. Examination of Firefly and Renilla Luciferase Activities in AGEs-Exposed Human Macrophages Following Plasmid Transfection. (A) Bar graphs present the measured Firefly (left panel) and Renilla (right panel) luciferase activities in human macrophages exposed to 10.0 μg/mL AGEs post-transfection with the bicistronic reporter plasmids, pR-dll4-F and δpR-dll4-F. The luciferase activities provide insights into the translational regulatory roles of the inserted Dll4 5′UTR fragments in these constructs under the influence of AGEs. **(B)** Similar to panel A, the depicted bar graphs represent the luciferase activities, both Firefly (left panel) and Renilla (right panel), in AGEs-exposed human macrophages post-transfection with pR-dll4-F and hpR-dll4-F plasmids. The differential activities between these two plasmids suggest nuances in the IRES-mediated translation due to the inclusion of the hairpin structure in the hpR-dll4-F construct. (n = 6, *P < 0.05, **P < 0.01, ***P < 0.001).

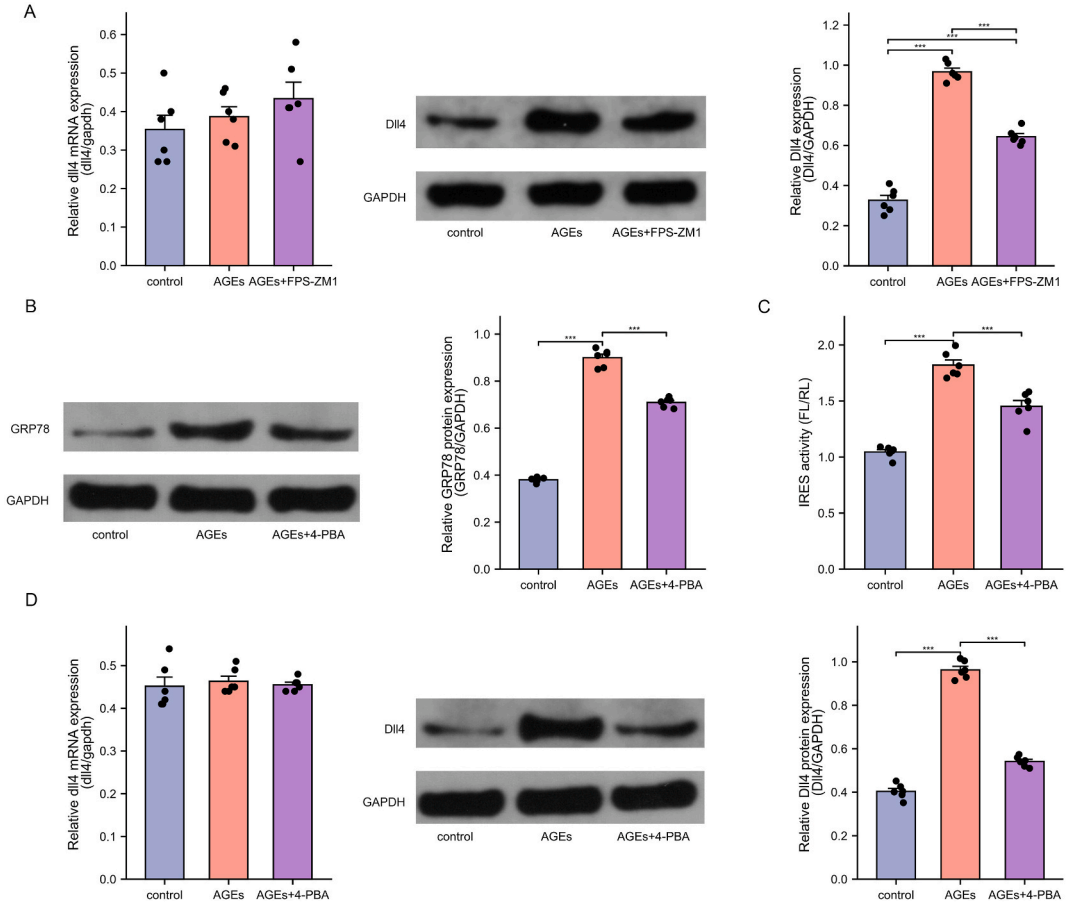

Fig. 5. Impact of FPS-ZM1 and 4-PBA Pre-treatments on Dll4 Expression and IRES Activity in AGEs-Exposed Human Macrophages. (A and FigureS2A) Left Panel: Bar graphs showcasing the relative dll4 mRNA expression levels in macrophages subjected to AGEs exposure (10.0 μg/mL) following a pre-treatment with the RAGE inhibitor, FPS-ZM1 (1.0 μmol/L). Right Panel: Accompanying immunoblots highlight the protein expression of Dll4 and the housekeeping protein, GRPDH. The succeeding bar graph quantifies the relative protein expression of Dll4 under the same treatment conditions. **(B** and FigureS2B) Left Panel: Immunoblots delineate the expression profiles of the ER stress marker, GRP78, and the control protein, GAPDH. Right Panel: Bar graphs quantify the relative GRP78 protein expression in macrophages exposed to AGEs (10.0 μg/mL) following a pre-treatment with the ER stress inhibitor, 4-PBA (1.0 mmol/L). **(C)** Bar graph representation of IRES-mediated translational activity (FL/RL ratio) observed in macrophages treated with AGEs (10.0 μg/mL) and a pre-treatment with 4-PBA (1.0 mmol/L). **(D** and FigureS2C) Left Panel: Columns depict the relative dll4 mRNA expression in macrophages subjected to AGEs exposure (10.0 μg/mL) with a pre-treatment of 4-PBA (1.0 mmol/L). Right Panel: Accompanying immunoblots exhibit protein expression levels of Dll4 and GAPDH, with subsequent bar graphs providing a quantitative assessment of the relative Dll4 protein expression under the stated conditions. (n = 6, *P < 0.05, **P < 0.01, ***P < 0.001).

4.5. ER stress PERK/eIF2α signaling was required for Dll4 5′UTR IRES activity

In order to evaluate the role of ER stress key pathway PERK/eIF2α signaling in AGEs- mediated Dll4 5′UTR IRES activity, siRNAs were used to silence PERK and eIF2α respectively. As demonstrated in Fig. 6A and B, perk-siRNA and eif2α-siRNA transfections significantly reduced PERK and eIF2α expressions as well as PERK and eIF2α phosphorylation in AGEs- exposed THP-1 cells. As a result, Dll4 expression was significantly down-regulated in AGEs-exposed THP-1 cells transfected with perk-siRNA or eif2α-siRNA. As shown in Fig. 6C, perk-siRNA and eif2α-siRNA transfections significantly decreased FL/RL in THP-1 cells exposed to AGEs. PERK/eIF2α signaling silencing significantly reduced Dll4 protein expression levels (Fig. 6E) without affecting dll4 mRNA expression levels (Fig. 6D). These results indicated that ER stress PERK/eIF2α pathway was indispensable in AGEs-mediated Dll4 5′UTR IRES activity.

4.6. PERK/eIF2α-mediated hnRNPA1 was the key ITAF for Dll4 IRES activity

The efficiency of IRES- dependent translation relies on ITAFs and their sub-cellular localization. hnRNPA1 is a typical ITAF regulating IRES activity. It was reported eIF2α activation facilitated the cytoplasmic re-localization of hnRNPA1 [14]. In this study, hnrnpa1-siRNA was synthesized to knock-down hnRNPA1 in THP-1 cells. The hnrnpa1-siRNA transfection effectively reduced hnRNPA1 expression (Fig. 7A), leading to dramatically reduced IRES activity in AGEs- exposed THP-1 cells (Fig. 7B). As shown in

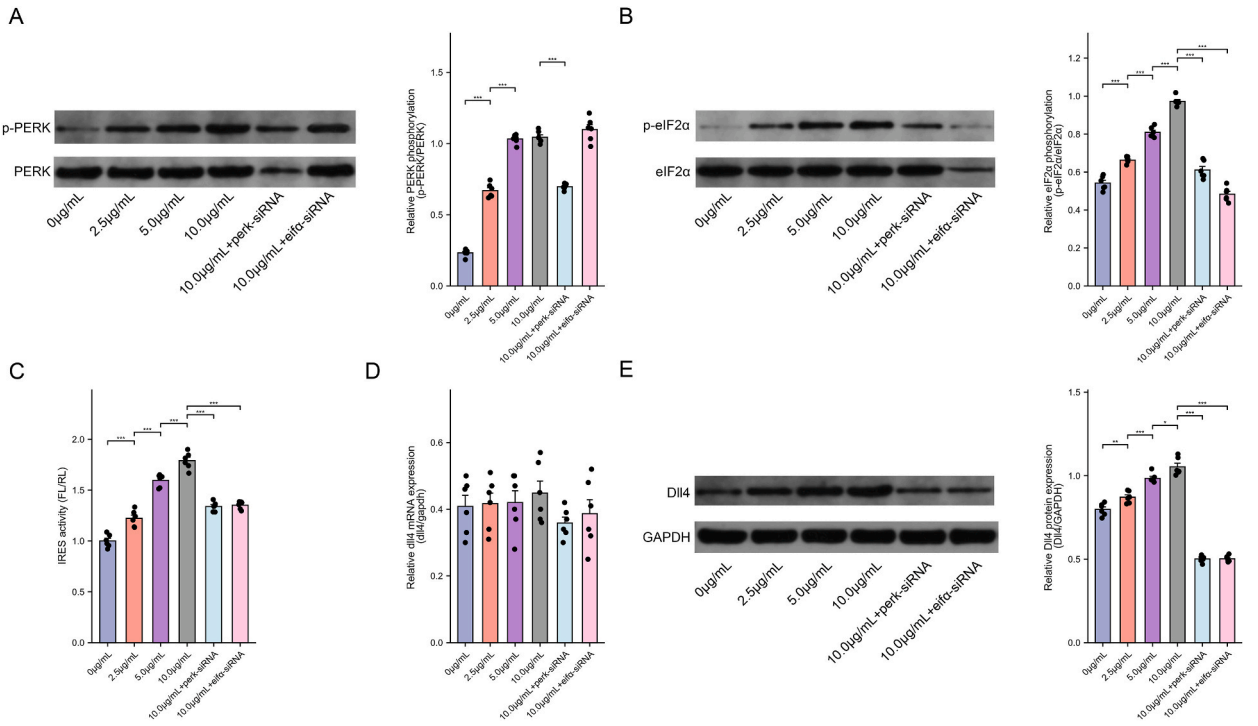

Fig. 6. Analysis of PERK and eIF2α Phosphorylation and Dll4 Expression in AGEs-Exposed Macrophages Following siRNA Transfections. (A and FigureS3A) Immunoblots display the protein profiles of phosphorylated PERK (p-PERK) and total PERK. Accompanying bar graphs quantify the relative phosphorylation levels of PERK in macrophages exposed to AGEs and transfected with either perk-siRNA or eif2α-siRNA. (**B** and FigureS3B) Immunoblots highlight the expression patterns of phosphorylated eIF2α (*p*-eIF2α) and total eIF2α. The subsequent bar graph offers a quantitative perspective on the relative phosphorylation levels of eIF2α under the described conditions. **(C)** Bar chart representation of the IRES-mediated translational activity associated with the Dll4 5′UTR in AGEs-exposed macrophages post-transfection with either perk-siRNA or eif2α-siRNA. **(D)** Columns delineate the relative mRNA expression levels of Dll4 in macrophages exposed to AGEs and transfected with the specified siRNAs, highlighting potential transcriptional modulations. **(E** and FigureS3C) Left Panel: Immunoblots present the protein expression spectra of Dll4 and the housekeeping protein, GAPDH. Right Panel: Corresponding bar graphs provide a quantitative assessment of the relative Dll4 protein expression in macrophages treated under the specified conditions, offering insights into the post-transcriptional regulatory roles of PERK and eIF2α in the context of AGEs exposure. (n = 6, *P < 0.05, **P < 0.01, ***P < 0.001).

Fig. 7C, both perk-siRNA and eif2α-siRNA transfections significantly facilitated re-localization of hnRNPA1 from nuclei to cytoplasm. As demonstrated in Fig. 7D, evidenced by co-localization analysis, both perk-siRNA and eif2α-siRNA transfections facilitated cytoplasmic accumulation of hnRNPA1 in AGEs- exposed THP-1 cells. These results suggested hnRNPA1 was the key ITAF for ER stress PERK/eIF2α pathway-mediated activity of IRES localized in Dll4 5′UTR.

5. Discussion

As important component of arterial vessels, VSMCs are located in the arterial media and take responsibilities in maintaining the structural and functional integrity of arteries. Phenotypic conversion from contractile phenotype to synthetic phenotype takes place when VSMCs are challenged by harmful stimuli. The phenotypic conversion is critical in formation and progression of atherosclerosis [15]. Our and others' previous investigation suggested Dll4/Notch signaling was responsible for the phenotypic conversion of VSMCs [7,16].

Interestingly, we found Dll4 high expression was characterized in AGEs-exposed macrophages which further induce phenotypic conversion of VSMCs by direct cell-to-cell contact [17]. Notably, AGEs were proved to induce ER stress in macrophages [18]. Thus, it seems that the significant increase of Dll4 expression in AGEs-exposed macrophages is paradox since synthesis of most "housekeeping" proteins is paused under circumstance of sustained ER stress. Moreover, our findings illuminate an intriguing aspect of AGEs' impact on Dll4 expression in macrophages. While AGEs exposure remained inconsequential to dll4 mRNA levels, Dll4 protein expression was markedly influenced. This discordance between mRNA and protein expressions further stood out when RAGE inhibition via FPS-ZM1 led to diminished Dll4 protein levels, leaving mRNA untouched. Such observations propel us to consider nuanced post-transcriptional regulatory mechanisms, potentially steered by the IRES within the Dll4 5′UTR. This facet, especially pronounced under ER stress conditions, necessitates further exploration to uncover the intricate interplay between AGEs and the regulatory domains within Dll4. Thus, it is highly probable that there would be alternative mechanisms to bypass ER stress-inhibited canonical cap-dependent translation. In mammals, IRES located in 5′UTR of mRNA could initiate protein translation when cap-dependent mechanism is

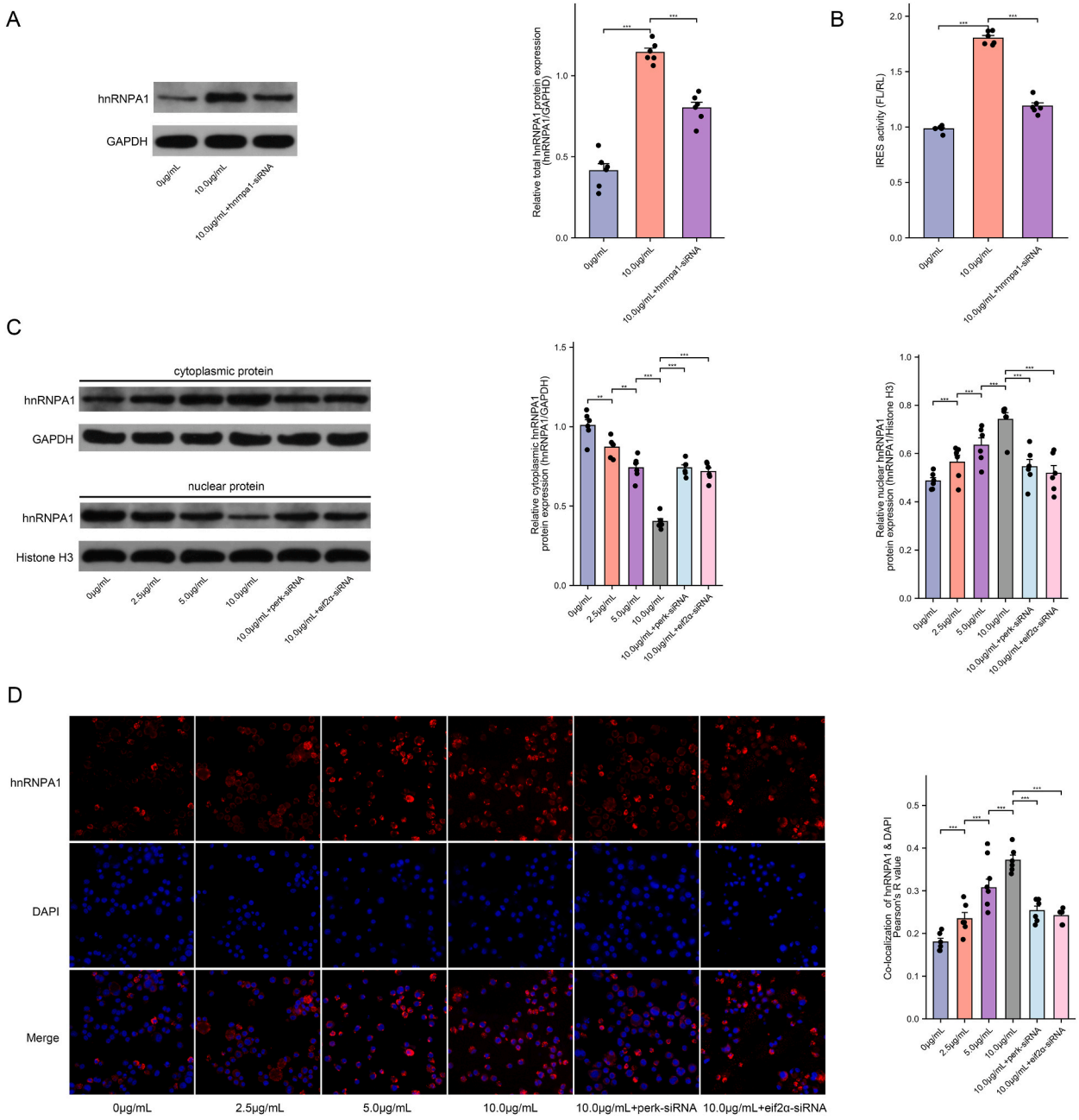

Fig. 7. Evaluating the Role of hnRNPA1 and its Subcellular Distribution in AGEs-Exposed Macrophages Following Transfections. (A and FigureS4A) Immunoblot analyses display the protein profiles of hnRNPA1 and the control, GAPDH, from total protein extracts. Accompanying bar graphs quantify the relative expression levels of total hnRNPA1 in macrophages exposed to AGEs and subsequently transfected with hnrnpa1-siRNA. **(B)** Bar charts showcase the IRES-mediated translational activity, represented as the FL/RL ratio, in AGEs-exposed macrophages post-transfection with hnrnpa1-siRNA. **(C)** Cytoplasmic Distribution: Immunoblots detail the expression patterns of hnRNPA1 and GAPDH from cytoplasmic protein extracts (FigureS4B). Bar graphs elucidate the relative expression levels of cytoplasmic hnRNPA1 in macrophages exposed to AGEs and transfected with either perk-siRNA or eif2α-siRNA. Nuclear Distribution: Immunoblots spotlight the expression of hnRNPA1 and the nuclear marker, Histone H3, from nuclear protein extracts (FigureS4C). Corresponding bar charts quantify the relative nuclear hnRNPA1 levels under the specified conditions. **(D)** Fluorescence microscopy images present immunostainings of hnRNPA1 (red) alongside DAPI-stained nuclei (blue) and their merged visualizations. Bar graphs offer a quantitative perspective, representing the Pearson's R value, which gauges the degree of co-localization between hnRNPA1 and DAPI in AGEs-exposed macrophages transfected with either perk-siRNA or eif2α-siRNA. ($n = 6$, $^{*}P < 0.05$, $^{**}P < 0.01$, $^{***}P < 0.001$).

globally suspended in cells under stressful conditions [19]. This mechanism could be a reasonable interpretation.

Glyceraldehyde-derived AGEs form a significant subset of AGEs, with established links to various pathologies, most notably diabetic complications. Our preparation of AGEs was comprised of glyceraldehyde-derived AGEs. The presence of these specific AGEs is crucial to consider, given their distinct biochemical properties and physiological effects. Drawing from literature, glyceraldehyde-derived AGEs have been implicated in cardiovascular disorders [20], reinforcing their role in the disease process. By using an AGE mixture with a substantial component of glyceraldehyde-derived AGEs, our study resonates with the broader clinical and pathophysiological context, further accentuating the significance of our findings in understanding the interplay between AGEs, ER stress, and Dll4 expression in macrophages. In this study, human macrophages were exposed to AGEs which triggered significant ER stress through RAGE. Dll4 protein expression was dramatically up-regulated whereas no significant change was found at transcriptional level. We noticed that the Dll4 5′UTR was GC rich and contained no upstream open reading frames. Moreover, stable and complex RNA secondary structures of Dll4 5′UTR were predicted. These structures could form a barrier to slow down the ribosome scanning. Thus, we proposed the existence of IRES in Dll4 5′UTR.

By using bicistronic reporter plasmid and dual-luciferase assay, we identified IRES activity in Dll4 5′UTR in human macrophages under ER stress induced by AGEs. Other mechanisms causing false positive dual-luciferase assay results including internal potential promoter and ribosomal read-through were excluded. The IRES activity often relies on ITAFs which promote ribosome recruitment by stabilizing adequate RNA conformation [21]. In this study, we found that targeted silencing of an ITAF, hnRNPA1, significantly inhibited Dll4 5′UTR IRES activity, indicating hnRNPA1 was an indispensable TIAF. Notably, it was reported that the activity of hnRNPA1 was dependent on eIF2α phosphorylation [14]. Our further study suggested targeted inhibition of PERK/eIF2α pathway deactivated hnRNPA1, resulting in significant reduced Dll4 5′UTR IRES activity.

In summary, under ER stress condition induced by AGEs exposure, IRES contained in Dll4 5′UTR enabled expression of Dll4 in human macrophages. Moreover, ER stress PERK/eIF2α signaling pathway mediated hnRNPA1 activation was indispensable for Dll4 5′UTR IRES activity.

Funding sources

This study was supported by National Natural Scientific Foundation of China (82070858); Chinese Medicine "Double Chain Integration" Youth Research and Innovation Team Project of Shaanxi Province (2022-SLRH-LJ-014); Qin Chuang Yuan Traditional Chinese Medicine Innovative R&D Project (2022-QCYZH-016); SPPH Scientific Research Supporting Projects (2021LJ-03, 2021BJ-02, 2021BJ-06, 2021YJY-02, 2021JY-18 and 2021YJY-08).

Data availability statement

No data been deposited into a publicly available repository. Data will be made available on request.

CRediT authorship contribution statement

Yanpeng Ma: Validation, Methodology, Investigation. **Shixiang Zheng:** Visualization, Resources, Investigation. **Xiqiang Wang:** Visualization, Methodology, Investigation, Data curation. **Ling Zhu:** Software, Methodology, Investigation, Formal analysis. **Junkui Wang:** Methodology, Investigation. **Shuo Pan:** Visualization, Investigation, Formal analysis, Data curation. **Yong Zhang:** Visualization, Validation, Methodology, Investigation. **Zhongwei Liu:** Writing – review & editing, Writing – original draft, Validation, Supervision, Resources, Project administration, Funding acquisition, Formal analysis, Data curation, Conceptualization.

Declaration of competing interest

The authors declare that they have no known competing financial interests or personal relationships that could have appeared to influence the work reported in this paper.

Appendix A. Supplementary data

Supplementary data to this article can be found online at https://doi.org/10.1016/j.heliyon.2023.e21170.

References

[1] Y. Xing, S. Pan, L. Zhu, Q. Cui, Z. Tang, Z. Liu, F. Liu, Advanced glycation end products induce atherosclerosis via RAGE/TLR4 signaling mediated-M1 macrophage polarization-dependent vascular smooth muscle cell phenotypic conversion, Oxid. Med. Cell. Longev. 2022 (2022), 9763377, https://doi.org/10.1155/2022/9763377.

[2] M. Viigimaa, A. Sachinidis, M. Toumpourleka, K. Koutsampasopoulos, S. Alliksoo, T. Titma, Macrovascular complications of type 2 diabetes mellitus, Curr. Vasc. Pharmacol. 18 (2020) 110–116, https://doi.org/10.2174/1570161117666190405165151.

[3] H. Vlassara, J. Uribarri, Advanced glycation end products (AGE) and diabetes: cause, effect, or both? Curr. Diabetes Rep. 14 (2014) 453, https://doi.org/10.1007/s11892-013-0453-1.

[4] F. Paneni, F. Cosentino, Advanced glycation endproducts and plaque instability: a link beyond diabetes, Eur. Heart J. 35 (2014) 1095–1097, https://doi.org/10.1093/eurheartj/eht454.
[5] I. Tabas, K.E. Bornfeldt, Macrophage phenotype and function in different stages of atherosclerosis, Circ. Res. 118 (2016) 653–667, https://doi.org/10.1161/circresaha.115.306256.
[6] G.J. Koelwyn, E.M. Corr, E. Erbay, K.J. Moore, Regulation of macrophage immunometabolism in atherosclerosis, Nat. Immunol. 19 (2018) 526–537, https://doi.org/10.1038/s41590-018-0113-3.
[7] Z. Liu, Y. Wang, H. Zhu, C. Qiu, G. Guan, J. Wang, Y. Guo, Matrine blocks AGEs- induced HCSMCs phenotypic conversion via suppressing Dll4-Notch pathway, Eur. J. Pharmacol. 835 (2018) 126–131, https://doi.org/10.1016/j.ejphar.2018.07.051.
[8] Z. Liu, Y. Ma, Q. Cui, J. Xu, Z. Tang, Y. Wang, C. He, X. Wang, Toll-like receptor 4 plays a key role in advanced glycation end products-induced M1 macrophage polarization, Biochem. Biophys. Res. Commun. 531 (2020) 602–608, https://doi.org/10.1016/j.bbrc.2020.08.014.
[9] Y.H. Chen, Z.W. Chen, H.M. Li, X.F. Yan, B. Feng, AGE/RAGE-Induced EMP release via the NOX-derived ROS pathway, Journal of diabetes research 2018 (2018), 6823058, https://doi.org/10.1155/2018/6823058.
[10] Y.S. Muthyalaiah, B. Jonnalagadda, C.M. John, S. Arockiasamy, Impact of Advanced Glycation End products (AGEs) and its receptor (RAGE) on cancer metabolic signaling pathways and its progression, Glycoconj. J. 38 (2021) 717–734, https://doi.org/10.1007/s10719-021-10031-x.
[11] J. Wu, R.J. Kaufman, From acute ER stress to physiological roles of the Unfolded Protein Response, Cell Death Differ. 13 (2006) 374–384, https://doi.org/10.1038/sj.cdd.4401840.
[12] Z. Liu, F. Fan, A. Wang, S. Zheng, Y. Lu, Dll4-Notch signaling in regulation of tumor angiogenesis, J. Cancer Res. Clin. Oncol. 140 (2014) 525–536, https://doi.org/10.1007/s00432-013-1534-x.
[13] J. Wang, R. Li, Z. Peng, B. Hu, X. Rao, J. Li, HMGB1 participates in LPS-induced acute lung injury by activating the AIM2 inflammasome in macrophages and inducing polarization of M1 macrophages via TLR2, TLR4, and RAGE/NF-κB signaling pathways, Int. J. Mol. Med. 45 (2020) 61–80, https://doi.org/10.3892/ijmm.2019.4402.
[14] E. Bevilacqua, X. Wang, M. Majumder, F. Gaccioli, C.L. Yuan, C. Wang, X. Zhu, L.E. Jordan, D. Scheuner, R.J. Kaufman, et al., eIF2alpha phosphorylation tips the balance to apoptosis during osmotic stress, J. Biol. Chem. 285 (2010) 17098–17111, https://doi.org/10.1074/jbc.M110.109439.
[15] M.R. Bennett, S. Sinha, G.K. Owens, Vascular smooth muscle cells in atherosclerosis, Circ. Res. 118 (2016) 692–702, https://doi.org/10.1161/circresaha.115.306361.
[16] A.J. Pedroza, T. Koyano, J. Trojan, A. Rubin, I. Palmon, K. Jaatinen, G. Burdon, P. Chang, Y. Tashima, J.Z. Cui, et al., Divergent effects of canonical and non-canonical TGF-β signalling on mixed contractile-synthetic smooth muscle cell phenotype in human Marfan syndrome aortic root aneurysms, J. Cell Mol. Med. 24 (2020) 2369–2383, https://doi.org/10.1111/jcmm.14921.
[17] Y. Ma, Y. Zhang, C. Qiu, C. He, T. He, S. Shi, Z. Liu, Rivaroxaban suppresses atherosclerosis by inhibiting FXa-induced macrophage M1 polarization-mediated phenotypic conversion of vascular smooth muscle cells, Frontiers in cardiovascular medicine 8 (2021), 739212, https://doi.org/10.3389/fcvm.2021.739212.
[18] R.T. Iborra, A. Machado-Lima, L.S. Okuda, P.R. Pinto, E.R. Nakandakare, U.F. Machado, M.L. Correa-Giannella, R. Pickford, T. Woods, M.A. Brimble, et al., AGE-albumin enhances ABCA1 degradation by ubiquitin-proteasome and lysosomal pathways in macrophages, J. Diabetes Complicat. 32 (2018) 1–10, https://doi.org/10.1016/j.jdiacomp.2017.09.012.
[19] R. Marques, R. Lacerda, L. Romão, Internal ribosome entry site (IRES)-Mediated translation and its potential for novel mRNA-based therapy development, Biomedicines 10 (2022), https://doi.org/10.3390/biomedicines10081865.
[20] S.H. Hooshiar, H. Esmaili, A. Taherian, S. Jafarnejad, Exercise, advanced glycation end products, and their effects on cardiovascular disorders: a narrative review, Heart and Mind 6 (2022) 139–150, https://doi.org/10.4103/hm.hm_31_22.
[21] M.D. Faye, M. Holcik, The role of IRES trans-acting factors in carcinogenesis, Biochim. Biophys. Acta 1849 (2015) 887–897, https://doi.org/10.1016/j.bbagrm.2014.09.012.